Distributed Control of Cyclic Formations with Local Relative Position Measurements

Kaveh Fathian, Dmitrii I. Rachinskii, Tyler H. Summers, Nicholas R. Gans

Abstract— **We propose a distributed control scheme for cyclic formations of multi-agent systems using relative position measurements in local coordinate frames. It is assumed that agents cannot communicate with each other and do not have access to global position information. For the case of three and four agents with desired formation defined as a regular polygon, we prove that under the proposed control, starting from almost any initial condition, agents converge to the desired configuration. Moreover, it is shown that the control is robust to the failure of any single agent. From Monte Carlo analysis, a conjecture is proposed to extend the results to any number of agents.**

Index Terms— **Position based formation, cyclic graph, distributed control, global stablility.**

I. Introduction

Distributed formation control of multi-agent systems can be defined as assigning control laws to individual agents in a network, such that agents collaboratively achieve a desired geometric formation. Distributed formation control has applications in ground and/or aerial vehicle formations [1], automated highway systems [2], cooperative robot manipulation, and modular robotics self configurations [3], to name a few.

If agents can measure the position of their neighbors in global or aligned local coordinate frames, existing methods [4], [5] assure global convergence to any feasible desired formation. However, oftentimes position measurements are *relative*, and are obtained in *unaligned local* coordinate frames. Furthermore, agents may not be able to communicate among themselves. In such cases, the formation control problem is significantly more complicated.

The majority of the work on formation control with local relative position measurements focuses on the desired formations that are defined in terms of inter-agent distances (distance-based control) [6]–[8], or angles (bearing-based control) [9]–[11]. Sensors that are used in practice such as ladar, radar, sonar, stereo cameras, etc., provide both angle and distance information, for which desired values can be defined. Therefore, desired formations defined in terms of both distances and bearings have been recently considered in the literature [12], [13]. Our focus in this work is such desired formations.

This work was supported by the US Air Force Research Laboratory award number FA8651-13-1-0003, NSF grant DMS-1413223, and DGIST R&D Program of the Ministry of Science and Technology of Korea (15-BD-01).

K. Fathian and N.R. Gans are with the Department of Electrical Engineering, D. I. Rachinskii is with the Department of Mathematical Sciences, T. H. Summers is with the Department of Mechanical Engineering, University of Texas at Dallas, Richardson, TX, 75080 USA. E-mail: {kaveh.fathian, ngans, dmitry.rachinskiy, tyler.summers}@utdallas.edu.

The sensing topology among the agents is another factor that can make the formation control more challenging. If the sensing topology is rich enough, any feasible desired formation can be achieved globally. For instance, we have shown in [13] that a sufficient condition for global stability is that the sensing graph contains a spanning subgraph with hierarchical structure[1]. On the other hand, sensing graphs that are cyclic do not satisfy the previous condition, and finding a control law with global convergence in such cases is still an open problem in its full generality. Therefore, analyzing cyclic formations is an important step toward finding control schemes that work for an arbitrary sensing topology.

In this work, we consider formation control of multi-agent systems with cyclic sensing graph and relative local position measurements. We focus on desired formations that are regular polygons, and propose a distributed control law to achieve the desired formation. We prove for the case of three and four agents that the control almost globally stabilizes the agents to the desired formation. Furthermore, from Monte Carlo analysis we conjecture that the results can be extended to any number of agents.

The main contribution of this work is the almost global stability of cyclic formations with desired formations defined in *both* distances and bearings. We are not aware of any previous work under these conditions. For *bearing-only* desired formations, [14] and [15] have proposed control laws for the case of 3 and 4 agents, respectively, that are globally convergent. Work by [16] proposed a control law for any number of agents that is locally convergent. Thus, agents may not converge to the desired shape if the initial configuration is not near the desired formation. Notice that it is not possible to control the scale of a configuration with bearing-only measurements. For cyclic *distance-only* desired formations, [17] has proposed a control scheme to stabilize the agents to a regular polygon. The convergence is local since there are initial conditions for which the system converges to a *stable* undesired equilibrium. In the case of distance-based desired formation, work done in [18], [19] has shown that a continuous, decentralized, and globally stable control may fail to exist for systems with 4 or more agents that contain cycles. Notice that it is not possible to distinguish a formation from its reflection using distance-only measurements. Lastly, note that in the problem of cyclic pursuit [20], [21], the control is a function of the relative position vectors that

[1] To be specific, it is sufficient if a spanning subgraph exists for which the associated Laplacian matrix is upper triangular and has two -1 elements in the i-th column, $i \geq 3$.

are measured in a *global* coordinate frame. In this work, all position measurements are relative and *local*. If agents can sense the position of a common target or neighbor, relative *local* position measurements suffice to achieve the cyclic pursuit [22]. Here, agents do *not* have a common neighbor.

The organization of the paper is as follows. The notation and assumptions are introduced in Section II. Background materials that are needed throughout the proofs are presented in Section III. The control law is introduced is Section IV. The stability analysis in the case of three and four agents are presented in Sections V and VI, respectively. Lastly, in Section VII it is shown that the control law can be used for more agents.

II. Notation and Assumptions

Let $\mathbb{Z}_n := \{0, 1, ..., n-1\}$ represent the set of n distinguished agents. We describe the sensing topology among the agents by a directed graph. Each vertex of the graph represents an agent. A directed edge from vertex $k \in \mathbb{Z}_n$ to $i \in \mathbb{Z}_n$ indicates that agent k can measure the relative position of agent i in its local coordinate frame. In such a case, agent i is called a neighbor of agent k. Throughout the paper the following assumptions hold.

Assumption 1. *The positions of all agents are restricted to a plane. Agents are numbered, i.e., they are distinguished, and know the identification number of their neighbors.*

Assumption 2. *Agents can measure the relative position of their neighbors, i.e., they do not need to have an aligned or global coordinate frame.*

Assumption 3. *The sensing graph is cyclic, and agents are numbered such that agent k is neighbor with agents $k-1$ and $k+1$ (modulo n), as shown in Fig. 1.*

Assumption 4. *The parameters that specify desired distances and angles are assumed to uniquely define a realizable shape (unique up to rotations and translations on the plane). The desired distances are assumed to be strictly positive.*

Assumption 5. *Agents are treated as points on the plane, and collision avoidance is not considered.*

Assumption 6. *The agents have single-integrator holonomic dynamics*

$$\dot{p}_k = u_k \tag{1}$$

where $p_k \in \mathbb{R}^2$ is the position of agent k, and $u_k \in \mathbb{R}^2$ is the control input to be determined.

Distance between agents i and j is denoted by d_{ij}, and the desired distance by d^*_{ij}. If agent k has neighbors i and j, we denote by θ_k the angle $\angle ikj$ measured counterclockwise, and by θ^*_k the desired angle. The set of non-negative real numbers is denoted by $\mathbb{R}^+$.

III. Background

Throughout the paper we will use the following definitions and lemmas (see [23] for more details).

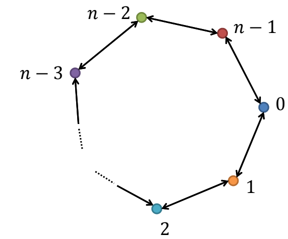

Fig. 1. Cyclic formation of n agents on the plane. Agent $k \in \mathbb{Z}_n$ can measure the relative position of its neighbors, agents $k-1$ and $k+1$.

Definition 1. *Consider the dynamical system $\dot{x} = F(x)$ with equilibrium $\bar{x}$, initial state x_0, and flow $\Phi(t,x)$. We say that $\bar{x}$ is almost globally stable if the set $\{x_0 : \lim_{t\to\infty} \Phi(t,x_0) \neq \bar{x}\}$ has zero Lebesgue measure. That is, trajectories converge to the equilibrium from almost all initial conditions.*

Definition 2. *Let F be continuously differentiable. A point $x^* \in \mathbb{R}^2$ is called a ω-limit point of a trajectory of $\dot{x} = F(x)$ if there exists a sequence of times $\{t_k\}_{k=1}^{\infty}$ such that $t_k \to \infty$ and $x(t_k) \to x^*$. The set of all ω-limit points is called the ω-limit set.*

Poincaré-Bendixson Theorem. Let $F : \Omega \to \mathbb{R}^2$ be continuously differentiable on $\Omega \subset \mathbb{R}^2$, where Ω is positive invariant and contains only finitely many equilibria. Suppose an ω-limit set of a trajectory belongs to a closed set $B \subset \Omega$. Then the ω-limit set is either

- a single equilibrium point,
- a periodic trajectory,
- a set of equilibrium points together with homoclinic or heteroclinic orbits connecting them.

Gronwall's Lemma. Let $x \in C^1([a,\infty))$, $f \in C^0([a,\infty))$, be such that $\dot{x} \leq f(t)x$ for all $t \in [a,\infty)$. Then,

$$x(t) \leq x(a)\, e^{\int_a^t f(\tau)d\tau}, \quad t \geq a. \tag{2}$$

In particular, if $\int_a^\infty f(\tau)d\tau = -\infty$, there exists $\varepsilon : [a,\infty) \to \mathbb{R}^+$, given by $\varepsilon(t) := |x(a)| \exp \int_a^t f(\tau)d\tau$, such that

$$x(t) \leq \varepsilon(t), \quad \lim_{t\to\infty} \varepsilon(t) = 0. \tag{3}$$

Note that when it is clear from the context, we omit the time dependency of variables for conciseness, e.g., we write x instead of $x(t)$.

Lemma 1. *Let $x \in C^1([a,\infty))$, $f, g \in C^0([a,\infty))$, be such that*

$$\dot{x} = f(t)x + g(t), \tag{4}$$

and assume that $f(t) < 0$, $g(t) \geq 0$, for every $t \in [a,\infty)$. Moreover, assume that $\int_a^\infty f(\tau)d\tau = -\infty$. Assume that

$$M := \limsup_{t\to\infty} \left(\frac{g(t)}{-f(t)} \right) < \infty. \tag{5}$$

Then, there exists $\varepsilon(t) \geq 0$ such that

$$x(t) \leq M + \varepsilon(t), \quad \lim_{t\to\infty} \varepsilon(t) = 0. \tag{6}$$

Proof. Due to assumption $f(t) < 0$, from (4) and (5) for any $\tilde{M} > M$ there exists a $t_0 \in [a,\infty)$ such that for all $t > t_0$

$$\dot{x} = f(t)(x - \frac{g(t)}{-f(t)}) \leq f(t)(x - \tilde{M}). \tag{7}$$

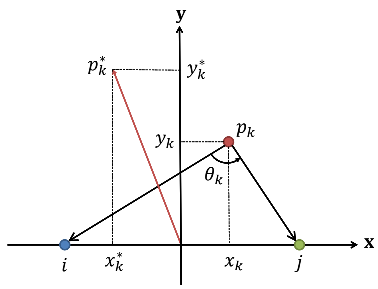

Fig. 2. Agent k with neighbors $i = k-1$ and $j = k+1$. To simplify the analysis, the local coordinate frame of agent k is transformed such that its origin is located at the midpoint of the line segment ij with the positive x-direction along the vector connecting i to j.

Since $\tilde{M}$ is constant, this implies

$$\frac{d(x-\tilde{M})}{dt} \leq f(t)(x-\tilde{M}). \tag{8}$$

Since $\int_a^\infty f(\tau)d\tau = -\infty$, by Gronwall's Lemma we conclude from (8) that $x(t) - \tilde{M} \leq \varepsilon(t)$ and because $\tilde{M} > M$ is arbitrary, (6) follows. □

IV. Control Law

Consider n agents with a cyclic sensing graph. By Assumption 3, agent k has neighbors $k-1$ and $k+1$. Define the shorthand notations $i := k-1$ and $j := k+1$ to denote the neighbors. Without loss of generality, pick the origin of agent k's local coordinate frame at the midpoint of the line segment connecting i to j, with the positive x-direction from i to j, as shown in Fig. 2. If at any time i and j coincide, the x-direction is chosen along any arbitrary direction. Notice that since agent k can measure the relative positions of agents i and j, its current local coordinate frame can be transformed to the aforementioned frame. This specific choice of coordinate simplifies the subsequent analysis.

Consider the *local* coordinate frame of agent k. Let p_i and p_j show the coordinates of the neighbors, and $p_k := [\bar{x}_k,\ \bar{y}_k]^T$ show the coordinate of agent k in this coordinate frame. Using the notations introduced in Section II, if the neighbors are at the desired distance from one another (i.e., $d_{ij} = d_{ij}^*$), then the distance and angle equalities $d_{ik} = d_{ik}^*$, $d_{jk} = d_{jk}^*$ and $\theta_k = \theta_k^*$ determine the desired position of agent k. Indeed, from the distance equalities we have

$$\|p_k - p_i\| = d_{ik}^*, \quad \|p_k - p_j\| = d_{jk}^*, \tag{9}$$

which since $p_i = [-\frac{d_{ij}^*}{2},\ 0]^T$ and $p_j = [\frac{d_{ij}^*}{2},\ 0]^T$ results in

$$(\bar{x}_k + \frac{d_{ij}^*}{2})^2 + \bar{y}_k^2 = {d_{ik}^*}^2, \quad (\bar{x}_k - \frac{d_{ij}^*}{2})^2 + \bar{y}_k^2 = {d_{jk}^*}^2. \tag{10}$$

Subtracting the equations in (10) yields

$$\bar{x}_k = \frac{1}{2d_{ij}^*}({d_{ik}^*}^2 - {d_{jk}^*}^2). \tag{11}$$

Note that since $d_{ij}^* > 0$ by Assumption 4, $\bar{x}_k$ is well defined.

The area of the parallelogram formed by vectors $p_k - p_i$ and $p_k - p_j$ is given by $d_{ik}d_{jk}\sin(\theta_k)$, and is equal to the determinant of the matrix formed by the vectors. Thus, from distance and angle equalities we have

$$\det([p_k - p_i,\ p_k - p_j]) = d_{ik}^* d_{jk}^* \sin(\theta_k^*), \tag{12}$$

which after simplifications results in

$$\bar{y}_k = \frac{1}{d_{ij}^*} d_{ik}^* d_{jk}^* \sin(\theta_k^*). \tag{13}$$

By Assumption 4, y_k is well defined.

Using the right hand sides of (11) and (13), define the vector of the desired location by

$$p_k^* := \begin{bmatrix} x_k^* \\ y_k^* \end{bmatrix} := \frac{1}{2d_{ij}^*} \begin{bmatrix} {d_{ik}^*}^2 - {d_{jk}^*}^2 \\ 2d_{ik}^* d_{jk}^* \sin(\theta_k^*) \end{bmatrix}. \tag{14}$$

Note that p_k^* is a constant vector determined by the distances and angle in the desired formation. We define the control law u_k in agent k's local coordinate frame by

$$u_k := -p_k + p_k^*. \tag{15}$$

The control law u_k navigates agent k to the desired position, which is the end point of the vector p_k^*, as shown in Fig. (2).

To analyze the stability of the system under the local control law (15), we need to represent the dynamics in a global coordinate frame. We assume from now on that $q_k := [x_k,\ y_k]^T$ represents the coordinates of agent $k \in \mathbb{Z}_n$ in an arbitrary *global* coordinate frame (which is unknown to agents). Let φ_{ji} be the angle that vector $q_j - q_i$ makes with the x-axis of the global coordinate frame, measured counterclockwise. From (1) and the local control law (15), the dynamics of agent k in the global coordinate frame is

$$\dot{q}_k = -q_k + \frac{1}{2}(q_j + q_i) + R_{ji}\ p_k^* \tag{16}$$

where p_k^* is the constant vector defined in (14), and the rotation matrix $R_{ji} \in \mathrm{SO}(2)$ is defined as

$$R_{ji} := \begin{bmatrix} \cos(\varphi_{ji}) & -\sin(\varphi_{ji}) \\ \sin(\varphi_{ji}) & \cos(\varphi_{ji}) \end{bmatrix} = \frac{1}{d_{ji}} \begin{bmatrix} x_j - x_i & -y_j + y_i \\ y_j - y_i & x_j - x_i \end{bmatrix}. \tag{17}$$

From (17), we can write (16) as

$$\dot{q}_k = -q_k + \frac{1}{2}(q_j + q_i) + \frac{1}{d_{ji}} H_k^* (q_j - q_i), \quad H_k^* := \begin{bmatrix} x_k^* & -y_k^* \\ y_k^* & x_k^* \end{bmatrix} \tag{18}$$

where $H_k^* \in \mathbb{R}^{2\times 2}$ is a constant matrix in terms of the desired coordinates (14). Notice for desired formations defined as regular polygons, $x_k^* = 0,\ y_k^* := h^*$ for all $k \in \mathbb{Z}_n$. Thus,

$$H_k^* := \begin{bmatrix} 0 & -h^* \\ h^* & 0 \end{bmatrix}. \tag{19}$$

V. Stability Analysis for 3 Agents

Stability analysis of the control scheme proceeds by proving the following theorem.

Theorem 1. *Consider a cyclic formation of 3 agents with an equilateral triangle as the desired formation. Under the control law* (15)*, the desired formation is almost globally stable, and the control is robust to the failure of any single agent.*

We start the proof with the case when 2 agents can move and show the robustness to the failure of any single agent. We then extend the proof idea to the case where all 3 agents move.

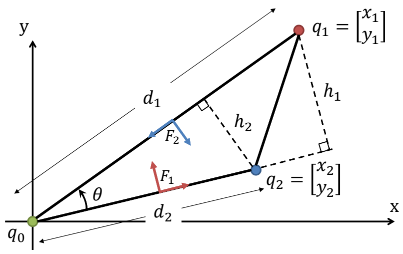

Fig. 3. Configuration of 3 agents on the plane with agent 0 located at the origin. Scalar $d_k := \|q_k\| \in \mathbb{R}^+,\ k \in \{1,2\}$, represents the side length. Scalar $h_k \in \mathbb{R}$ represents the signed height subtended at agent k, and is equal to the y-coordinate of agent k in its local coordinate frame, F_k.

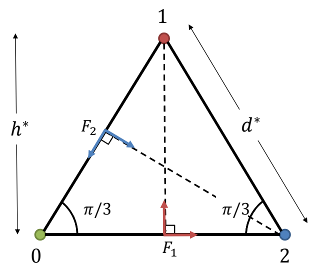

Fig. 4. Equilateral desired formation, with $d^* > 0$ and $h^* > 0$ representing the desired side lengths and heights, respectively. The local coordinate frames of agents 1 and 2 are shown by F_1 and F_2, respectively.

A. Robustness to Failure of One Agent

The organization of the proof is as follows. We first introduce the variables that are used in the analysis and show that they are bounded along the trajectories of the system. We then show that all trajectories converge to the invariant manifold on which the distance between each moving agent and the fixed agent is equal. The proof proceeds by showing that starting from almost any initial condition, the signed area of the triangle formed by the agents becomes strictly positive in finite time and stays strictly positive thereafter. That is, when agents start from the wrong orientation, they achieve the correct orientation in finite time. Lastly, under the assumption that the signed area is positive, we apply the Poincaré-Bendixson Theorem and show that agents achieve the desired formation.

Denote the coordinates of agent $k \in \mathbb{Z}_3$ by $q_k := [x_k, y_k]^T$ in the *global* coordinate frame, as shown in Fig. 3. Without loss of generality, assume that agent 0 is fixed at the origin and cannot move. Denote the angle between vectors q_2 and q_1 (measured counterclockwise) by $\theta \in (-\pi, \pi]$, and define $d_1 := \sqrt{x_1^2 + y_1^2}$, $d_2 := \sqrt{x_2^2 + y_2^2}$ as the length of the vectors q_1 and q_2, respectively. The desired formation is shown in Fig. 4. The desired height and side length are shown by h^* and d^*, respectively. We assume that h^* is positive and define the desired signed area of the triangle by $A^* := \frac{1}{2} h^* d^*$. Note that the signed height (and area) is what distinguishes a formation from its reflection.

Substituting H_k^*, given by (19), and $q_0 = [0, 0]^T$ in (18), dynamics of the agents in the global coordinate frame are given by

$$\begin{aligned} \dot{x}_1 &= -x_1 + \frac{1}{2}x_2 - \frac{h^*}{d_2}y_2, \\ \dot{y}_1 &= -y_1 + \frac{1}{2}y_2 + \frac{h^*}{d_2}x_2, \\ \dot{x}_2 &= -x_2 + \frac{1}{2}x_1 + \frac{h^*}{d_1}y_1, \\ \dot{y}_2 &= -y_2 + \frac{1}{2}y_1 - \frac{h^*}{d_1}x_1. \end{aligned} \tag{20}$$

*1) **Required Variables:*** Define the sum of side lengths and its desired value by $P := d_1 + d_2 \in \mathbb{R}^+$, and $P^* := 2d^*$, respectively. Computing $\dot{P}$ along the trajectories of (20) yields

$$\dot{P} = \frac{2h^*}{d_1 d_2}(x_2 y_1 - x_1 y_2) + \frac{d_1 + d_2}{2 d_1 d_2}(x_1 x_2 + y_1 y_2) - (d_1 + d_2). \tag{21}$$

Noting that

$$x_2 y_1 - x_1 y_2 = \det([q_2,\ q_1]) = d_1 d_2 \sin(\theta), \tag{22}$$

$$x_1 x_2 + y_1 y_2 = \mathrm{dot}(q_2,\ q_1) = d_1 d_2 \cos(\theta), \tag{23}$$

and since $h^* = \frac{\sqrt{3}}{2} d^*$ in an equilateral triangle, we can simplify (21) as

$$\dot{P} = \left(\frac{\cos(\theta)}{2} - 1 \right) P + \frac{\sqrt{3}\sin(\theta)}{2} P^*. \tag{24}$$

Since $\frac{\cos(\theta)}{2} - 1 \le \frac{-1}{2}$, by Lemma 1 we conclude from (24) that there exists $\varepsilon(t) \ge 0$ such that $\varepsilon(t) \to 0$ and

$$P(t) \le \limsup_{t \to \infty} \left(\frac{\frac{\sqrt{3}\sin(\theta)}{2}}{1 - \frac{\cos(\theta)}{2}} P^* \right) + \varepsilon(t) = P^* + \varepsilon(t). \tag{25}$$

Note that the argument of lim sup in (25) achieves its maximum at $\theta = \frac{\pi}{3}$. Positivity of distances together with (25) implies

$$0 \le P(t) \le P^* + \varepsilon(t). \tag{26}$$

Therefore, we have shown that P is upper bounded in the limit by its desired value, P^*, as $t \to \infty$.

Let $A \in \mathbb{R}$ be the signed area of the triangle, defined by

$$A := \frac{1}{2}\det([q_2,\ q_1]) = \frac{1}{2}(x_2 y_1 - x_1 y_2) = \frac{1}{2} d_1 d_2 \sin(\theta).$$

From (20) we get

$$\dot{A} = x_1 y_2 - x_2 y_1 + \frac{h^*}{2d_1}(x_1^2 + y_1^2) + \frac{h^*}{2d_2}(x_2^2 + y_2^2). \tag{27}$$

Since $d_k^2 = x_k^2 + y_k^2,\ k \in \{1,2\}$, (27) simplifies to

$$\dot{A} = -2A + \frac{h^*}{2}P. \tag{28}$$

Substituting P by its upper bound (26) and noting that $h^* P^* = 2A^*$ we have

$$\dot{A} \le -2A + 2A^* + \frac{h^* \varepsilon(t)}{2}. \tag{29}$$

Note that A^*, h^*, ε are non-negative, and $\varepsilon \to 0$. Thus, by Lemma 1, (29) implies

$$A(t) \le A^* + \varepsilon'(t), \tag{30}$$

where ε' is positive and $\varepsilon' \to 0$.

Other dynamics that are required in the analysis are dynamics of d_1 and d_2, which are given by

$$\begin{aligned} \dot{d}_1 &= -d_1 + \frac{1}{2} d_2 \cos(\theta) + h^* \sin(\theta), \\ \dot{d}_2 &= -d_2 + \frac{1}{2} d_1 \cos(\theta) + h^* \sin(\theta), \end{aligned} \tag{31}$$

and θ, which is given by

$$\dot{\theta} = \frac{d_1 + d_2}{d_1 d_2} h^* \cos(\theta) - \frac{d_1^2 + d_2^2}{2 d_1 d_2} \sin(\theta). \tag{32}$$

Note that (32) is calculated by taking the time derivative of $A = \frac{1}{2} d_1 d_2 \sin(\theta)$, and substituting $\dot{A}, \dot{d}_1, \dot{d}_2$ from (28) and (31).

*2) **The Invariant Manifold**:* We now show that all trajectories of (20) are attracted to the invariant manifold $d_1 = d_2$. Define $E \in \mathbb{R}^+$ as $E := \frac{1}{2}(d_1 - d_2)^2$. From (31) we have

$$\dot{E} = (-2 - \cos(\theta)) E \quad \leq \quad -E. \tag{33}$$

Since E is bounded below by zero, by Gronwall's Lemma it follows that E converges to zero.

*3) **Lower Bounds for A and P**:* If agents start from the wrong orientation, i.e., $A(0) < 0$, it is shown in Appendix I that A becomes non-negative in a finite time $t = \tau$. Additionally, for almost all initial conditions either d_1 or d_2 are non-zero at time τ, which implies P is non-zero. Thus, from (28), A becomes strictly positive and remain positive thereafter. Note that once $P > 0, \; A > 0$, from Gronwall's Lemma (24) and (28) ensure that $P > 0, \; A > 0$ after this moment. Therefore, $d_1, d_2 > 0$ and $\theta \in (0, \pi)$ for all $t > \tau$.

Since for a given P the maximum area of triangle is achieved when $\theta = \frac{\pi}{2}$, we have $A \leq P^2$, from which by (28)

$$\dot{A} \geq -2A + \sqrt{A}. \tag{34}$$

Since $\sqrt{A} > 2A$ for small non-zero A, (34) implies that there exists $A_0 > 0$ such that $A(t) > A_0$ at some time. Therefore, from $A \leq P^2$, there exists $P_0 > 0$ such that $P(t) > P_0$. These lower bounds together with upper bounds (26) and (30) imply that there exists a finite time τ_0 such that for all $t > \tau_0$

$$P_0 \leq P \leq P^* + \varepsilon(t), \quad \theta_0 \leq \theta \leq \pi - \theta_0 \tag{35}$$

where $\varepsilon \to 0$ and $\theta_0 := \arcsin(\frac{A_0}{P^{*2}})$ is a positive constant. We are now ready to apply the Poincaré-Bendixson's Theorem.

*4) **Convergence to the Desired Shape**:* Since $d_1 = d_2$ is an invariant and attracting manifold for system (20), we can constrain the analysis to $d_1 = d_2 := d$. On this manifold, dynamics of $P = 2d$ and θ are given from (24) and (32) as

$$\begin{aligned} \dot{P} &= \left(\frac{\cos(\theta)}{2} - 1 \right) P + \frac{\sqrt{3} \sin(\theta)}{2} P^*, \\ \dot{\theta} &= \frac{4}{P} h^* \cos(\theta) - \sin(\theta). \end{aligned} \tag{36}$$

Since P is non-negative by definition, the only feasible equilibrium of (36) is $(P, \theta) = (P^*, \theta^*)$, where $\theta^* := \frac{\pi}{3}$. By applying Poincaré-Bendixson's Theorem to the intersection of the manifold $d_1 = d_2$ with the closed set (35), it follows that all trajectories converge to the desired equilibrium. Indeed, since any periodic orbit must contain the equilibrium point (P^*, θ^*), from $P \leq P^* + \varepsilon(t)$ and $\varepsilon \to 0$ we conclude that the ω-limit set of any trajectory should contain the equilibrium point (P^*, θ^*), or a homoclinic orbit. However, eigenvalues of the Jacobian matrix derived from linearizing the dynamics (36) at the desired equilibrium are $-\frac{3}{4}, -2$. Therefore, the equilibrium is locally stable and homoclinic orbits do not exist. Heteroclinic orbits do not exist since the closed region (35) contains only one equilibrium.

B. Stability Analysis for all 3 Agents Moving

When all 3 agents can move, dynamics in the global coordinate frame are given by (18), where d_{ij}'s represent the side lengths of the triangle. Denote the side lengths by d_{12}, d_{20} and d_{01}. Let $i = k-1, \; j = k+1$ be the neighbors of agent $k \in \mathbb{Z}_3$. It is straightforward to show that

$$\dot{d}_{ij} = -\frac{3}{2} d_{ij} + 2 \frac{d_{ki} + d_{kj}}{d_{ij} d_{ki} d_{kj}} A h^* \tag{37}$$

where A is the signed area of the triangle and is given by[2]

$$A = \frac{1}{2} \sum_{k \in \mathbb{Z}_3} \det([q_{k+1}, \; q_k]). \tag{38}$$

Denote the perimeter of the triangle by $P := d_{12} + d_{20} + d_{01} \in \mathbb{R}^+$, with desired value $P^* = 3d^*$. From (37) it follows that

$$\dot{P} = -\frac{3}{2} P + \frac{4 A h^*}{d_{12} d_{20} d_{01}} P. \tag{39}$$

Since the area of every triangle is upper bounded by

$$A \leq \frac{3\sqrt{3}}{4} \frac{d_{12} d_{20} d_{01}}{P} \tag{40}$$

with equality holding if and only if the triangle is equilateral [24], from (39) and using the relation $h^* = \frac{\sqrt{3}}{2} d^*$ we obtain

$$\dot{P} \leq -\frac{3}{2} P + \frac{3}{2} P^*. \tag{41}$$

From (41) and Lemma 1 we conclude that

$$0 \leq P(t) \leq P^* + \varepsilon(t), \tag{42}$$

where ε is a non-negative function that goes to zero. Note that the zero lower bound holds due to non-negativity of perimeter by definition.

Let $A^* := \frac{1}{2} h^* d^*$ represent the desired area. From (38), one can show that

$$\dot{A} = -3A + \frac{h^*}{2} P. \tag{43}$$

Substituting (42) in (43) and using Lemma 1 yields

$$-\varepsilon'(t) \leq A(t) \leq A^* + \varepsilon''(t), \tag{44}$$

where $\varepsilon', \varepsilon''$ are non-negative functions that go to zero.

Define $E := \frac{1}{2}(d_{ki} - d_{kj})^2$ for an arbitrary pair of side lengths d_{ki} and d_{kj}. Using (37) we derive

$$\dot{E} = -\left(3 + \frac{4 A h^*}{d_{12} d_{20} d_{01}} \right) E. \tag{45}$$

[2]Known as Gauss's area formula or the shoelace formula.

Due to non-negativity of distances, h^*, and A in the limit (as shown in (44)), we conclude from (45) and Gronwall's Lemma that E goes to zero. Thus, the length of all sides become equal in the limit. Since the manifold $d_{12} = d_{20} = d_{01} := d$ is invariant and attractive, we henceforth constrain the analysis to this manifold, on which $P = 3d$. Consequently, from (39) and (43) we derive the 2-dimensional system

$$\begin{aligned} \dot{P} &= -\frac{3}{2}P + \frac{108 A h^*}{P^2}, \\ \dot{A} &= -3A + \frac{h^*}{2}P. \end{aligned} \tag{46}$$

Since $P \geq 0$ by definition, the only feasible equilibrium of (46) is at $(P,A) = (P^*, A^*)$. From (42), (44), and Poincaré-Bendixson's Theorem it follows that all trajectories starting from a compact set $S := \{(P,A) : P \in [P_0, P^*], A \in [A_0, A^*],\ P_0, A_0 > 0\}$ converge to the desired equilibrium (P^*, A^*). From similar analysis to Section V-A, we can show that all trajectories should enter S in finite time, with the exception of only one trajectory that tends to $(P,A) = (0,0)$. Therefore the desired formation is almost globally stable.

VI. Stability Analysis for 4 Agents

We extend the results in previous section by proving the following theorem for 4 agents.

Theorem 2. *Consider a cyclic formation of 4 agents with control law* (15)*, and desired formation defined as a square. The desired formation is almost globally stable.*

The dynamics of the system in the global coordinate frame are given by (18), where d_{ij}'s represent the diagonals of the quadrilateral. Denote the diagonals by d_{13} and d_{20}. Notice that h^* represents half of the diagonal length in the desired square, as illustrated in Fig.5. From (18), it follows that

$$\begin{aligned} \dot{d}_{13} &= -d_{13} + \frac{4}{d_{13} d_{20}} A h^*, \\ \dot{d}_{20} &= -d_{20} + \frac{4}{d_{13} d_{20}} A h^*. \end{aligned} \tag{47}$$

Define $P := d_{13} + d_{20}$, and denote the desired value of P by $P^* := 4h^*$. From (47) we obtain

$$\dot{P} = -P + \frac{8}{d_{13} d_{20}} A h^*, \tag{48}$$

where A is the signed area of the quadrilateral and is defined as

$$A := \frac{1}{2} \sum_{k \in \mathbb{Z}_4} \det([q_{k+1},\ q_k]). \tag{49}$$

Since the area of any quadrilateral is upper bounded by $A \leq \frac{d_{13} d_{20}}{2}$, from (48) we derive

$$0 \ \leq\ P(t) \ \leq\ P^* + \varepsilon(t), \tag{50}$$

where $\varepsilon \to 0$ and is non-negative.

It is straightforward to show that

$$\dot{A} = -2A + h^* P, \tag{51}$$

from which by (50) we have

$$-\varepsilon'(t) \ \leq\ A(t) \ \leq\ A^* + \varepsilon''(t), \tag{52}$$

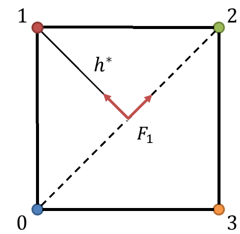

Fig. 5. Square desired formation, with $h^* > 0$ representing half of the diagonal length. The local coordinate frame of agents 1 is shown by F_1.

where ε', ε'' are non-negative functions that go to zero.

By defining $E := \frac{1}{2}(d_{13} - d_{20})^2$, we can show from (47) that $\dot{E} = -2E$, and therefore diagonals become equal in length in the limit $t \to \infty$. By constraining the analysis to the manifold $d_{13} = d_{20} := d$, we have $P = 2d$, and from (47) and (51)

$$\begin{aligned} \dot{P} &= -P + \frac{32 A h^*}{P^2}, \\ \dot{A} &= -2A + h^* P. \end{aligned} \tag{53}$$

The only feasible equilibrium of (53) is at $(P,A) = (P^*, A^*)$. From the Poincaré-Bendixson Theorem and similar analysis to Section V, it follows that P and A converge to their desired values for all but one of the trajectories. Formations satisfying $(P,A) = (P^*, A^*)$ form a 5-dimensional manifold $\mathcal{M}$ consisting of quadrilaterals with equal perpendicular diagonals of the desired length d^*. Thus, we have shown that $\mathcal{M}$ is an almost globally attractive manifold for the system. Notice that $(P,A) = (P^*, A^*)$ implies that $d = 2h^*$, from which $\frac{1}{d_{ji}} H_k^*$ is a skew-symmetric matrix with $\pm\frac{1}{2}$ off-diagonal elements. Thus, from (18) the dynamics on $\mathcal{M}$ are defined by the linear system

$$\begin{aligned} \dot{x}_k &= -x_k + \frac{1}{2}(x_j + x_i - y_j + y_i) \\ \dot{y}_k &= -y_k + \frac{1}{2}(y_j + y_i + x_j - x_i) \end{aligned}, \quad k \in \mathbb{Z}_4, \tag{54}$$

where $i = k-1$ and $j = k+1$. The eigenvalues of the linear system (54) on $\mathcal{M}$ are 0 of multiplicity four and -2. The 4-dimensional kernel corresponds to square formations and their rotations and translations. Therefore, (since $A = A^*$) we conclude that agents converge to the desired formation.

VII. Stability Analysis for 5 or More Agents

Analysis for 5 or more agents is challenging and will be a subject of future work. Nevertheless, based on Monte Carlo analysis with 10^6 random initial conditions for up to 20 agents, we propose the following conjecture.

Conjecture 1. *Under the control law* (15)*, any regular polygon is almost globally stable. Furthermore, the control is robust to the failure of one agent.*

Example 1. Consider cyclic formation of 10 agents with regular 10-gon as the desired formation. Assume that agents have initial random positions on the plane, as shown in Fig. 6(a) by circles. The control law (15) drives the agents to their final positions, shown by discs in the figure. Due to lack of global coordinate frame, agents achieve the desired formation

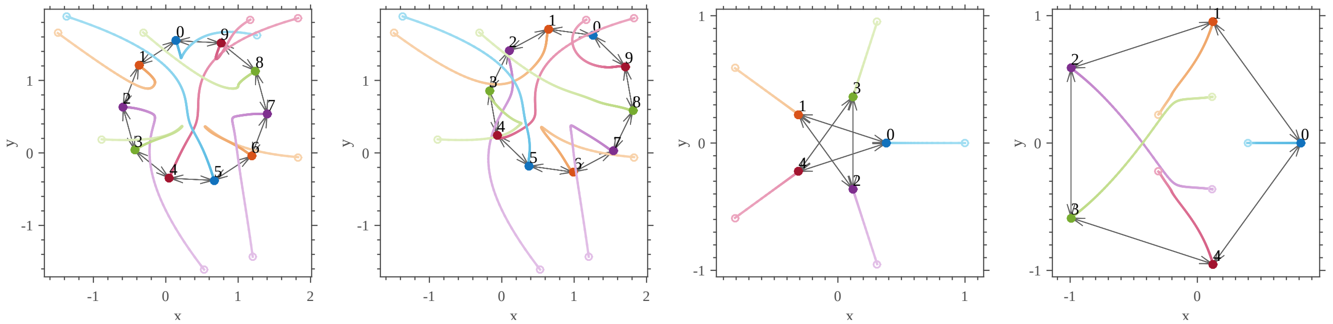

(a) (b) (c) (d)

Fig. 6. (a) Starting from random initial positions, shown by circles, the control law (15) drives the agents to their final position, shown by discs. The desired formation is a regular 10-gon. (b) Starting from the same initial conditions and under the assumption that agent 0 has failed to move and is fixed at its initial condition, the rest of the agents achieve the desired formation. (c) For 5 agents with regular pentagon desired formation, star configurations define an undesired, but unstable invariant manifold. (d) Small perturbation of agent 0 in the star configuration results is convergence to the desired formation. Simulation videos are available at https://youtu.be/XWoSKu29CUs .

up to rotations and translations. Under the assumption that agent 0 has failed to move and is fixed at its initial condition, Fig. 6(b) shows the trajectories of the agents starting from the same initial conditions. As can be seen from the figure, agents converge to the desired formation. The link to the simulation video can be found in the figure caption.

Example 2. Consider cyclic formation of 5 agents with desired formation defined as a regular pentagon. Due to the *almost* global stability property, these exists a measure zero set of initial conditions for which agents do not converge to the desired equilibrium. For example, Fig. 6(c) shows that star configurations define an invariant manifold, on which agents converge to an undesired equilibrium. One can show that Jacobian matrix has positive eigenvalue 0.339 of multiplicity two at the star equilibrium. Therefore, star is an unstable equilibrium. Indeed, Fig. 6(d) shows the trajectories when agent 0 is slightly perturbed. The perturbation causes the agents to converge to the desired formation.

VIII. Conclusions and Future Work

We proposed a distributed control law for cyclic formation of multi agent systems with relative position measurements. We proved for the case of 3 and 4 agents that desired formations defined as regular polygons are almost globally stable equilibria of the control law. Using Monte Carlo analysis, we proposed the conjecture that regular polygons are almost globally stable for any number of agents. Future work include proving the conjecture, and extending the results to a wider class of desired formations.

Appendix I
Convergence to Non-negative Area

Assume by contradiction that $A<0$ for all time. This implies that d_1, d_2 are non-zero, and $\theta \in (-\pi, 0)$ for all time. By (24) we conclude that $P \to 0$ as $t \to \infty$. Therefore, there exists $\varepsilon > 0$ and time τ such that $P \le \varepsilon$ for $t \ge \tau$. If for some $t \ge \tau$ we have $\cos(\theta) \le \frac{-\varepsilon}{h^*}$, then by (32) and since $P<\varepsilon$

$$\dot{\theta} \le \frac{-\varepsilon P}{d_1 d_2} - \frac{d_1^2+d_2^2}{2d_1d_2}\sin(\theta) \le \frac{-\varepsilon P}{d_1 d_2} + \frac{P^2}{2d_1d_2} \le \frac{-P^2}{2d_1d_2} \le \frac{-1}{2}. \tag{55}$$

Thus, θ monotonically decreases with velocity (at least) $-\frac{1}{2}$, which contradicts $\theta \in (-\pi,0)$ for all time (i.e., θ becomes $-\pi$ in finite time). Similarly, if $\cos(\theta) \ge \frac{-\varepsilon}{h^*}$, we derive $\dot{\theta} \ge \frac{1}{2}$ which is a contradiction. Thus, we must have that $|\cos(\theta)| \le \frac{\varepsilon}{h^*}$, but then $\sin(\theta) \approx 1$ and from (31) we get $\dot{d}_1 < \frac{-h^*}{2}$ and $\dot{d}_2 < \frac{-h^*}{2}$. This is a contradiction since either d_1 or d_2 become zero in finite time. Therefore we have shown that if agents start from the wrong orientation, the area becomes zero in finite time $t=\tau$. We now show that there is only one orbit with both $d_1(\tau)$ and $d_2(\tau)$ zero at time τ.

A. Case $d_1(0) \neq d_2(0)$

Notice that if $d_1(0) \neq d_2(0)$, from (33) we have $d_1 \neq d_2$ for all time. Indeed, from (33) we have $\dot{E} \ge -3E$, and from Gronwall's Lemma we have $E(\tau) \ge e^{-3\tau}E(0)$. Thus, if one of d_1, d_2 becomes zero at $t=\tau$, the other distance is non-zero at this time.

B. Case $d_1(0) = d_2(0)$

Notice that by (33), $d_1 = d_2$ for all time. Since $\dot{P} < 0$ for $t \in [0,\tau)$, from dividing (32) by (24) (with $d_1 = d_2 = \frac{P}{2}$) we have

$$\frac{d\theta}{dP} = f(P,\theta) := \frac{\frac{4}{P}h^*\cos(\theta) - \sin(\theta)}{(\frac{\cos(\theta)}{2}-1)P + 2h^*\sin(\theta)} \tag{56}$$

where we defined $f(P,\theta)$ as the right hand side of (56).

Assume $P \in (0,\varepsilon)$ for fixed $\varepsilon > 0$. We show that if $P \to 0$, then $\cos(\theta) \to 0$, i.e., $\theta \to \frac{-\pi}{2}$. Indeed, if $\cos(\theta) \ge \frac{\varepsilon}{h^*}$, by

$$\begin{aligned} \frac{4}{P}h^*\cos(\theta) &\ge \frac{4\varepsilon}{P}, & -\sin(\theta) &\ge 0, \\ \left(\frac{\cos(\theta)}{2}-1\right)P &\le P \le \varepsilon, & 2h^*\sin(\theta) &\le 2h^*, \end{aligned} \tag{57}$$

we have from (56) that

$$\frac{d\theta}{dP} \le -\frac{\frac{4\varepsilon}{P}}{\varepsilon + 2h^*} \le -\frac{4\varepsilon}{3h^* P}. \tag{58}$$

From (58) we have

$$\theta(\varepsilon)-\theta(P) \;\leq\; -\frac{4\varepsilon}{3h^*}\int_P^{\varepsilon}\frac{dP}{P} \;=\; -\frac{4\varepsilon}{3h^*}\ln\left(\frac{\varepsilon}{P}\right), \quad (59)$$

which implies

$$\theta(P) \;\geq\; \theta(\varepsilon)+\frac{4\varepsilon}{3h^*}\ln\left(\frac{\varepsilon}{P}\right), \quad (60)$$

and therefore $\theta(P)\to\infty$ as $P\to 0$. This shows that $\theta=0$ before P reaches zero. Note that once $\cos(\theta)\geq\frac{\varepsilon}{h^*}$ for some $t\in[0,\tau)$, from (32) we have

$$\dot{\theta} \;\geq\; \frac{4\varepsilon}{P}-\sin(\theta) \;\geq\; \frac{4\varepsilon}{P} > 0. \quad (61)$$

Thus, $\cos(\theta)$ remains larger than or equal to $\frac{\varepsilon}{h^*}$ thereafter. We conclude for any trajectory with $\cos(\theta)\geq\frac{\varepsilon}{h^*}$, at $t=\tau$ one of d_1, d_2 is greater than zero. Similar argument shows that for any trajectory with $\cos(\theta)\leq\frac{-\varepsilon}{h^*}$, $\theta=-\pi$ before P reaches zero. Since the analysis holds for all $\varepsilon>0$, any trajectory with $P\to 0$ has $\cos(\theta)\to 0$. It remains to show that there is only one trajectory for which $P\to 0$.

Suppose, by contradiction, that there exist two trajectories for which $P\to 0$. Let θ_1 and θ_2 represent the solutions of (56) for each trajectory for $P>0$. We should have $\theta_1,\theta_2\to\frac{-\pi}{2}$ as $P\to 0$. Without loss of generality, assume $\theta_1>\theta_2$, and define $\Delta\theta:=\theta_1-\theta_2$. Note that since $f(P,\theta)$ is Lipschitz for non-zero P, due to uniqueness of solutions θ_1 and θ_2 cannot collide at any other point than $\frac{-\pi}{2}$. From the mean value theorem, there exists $\tilde{\theta}(P)\in(\theta_2,\theta_1)$ such that

$$\frac{d\Delta\theta}{dP} \;=\; f(P,\theta_1)-f(P,\theta_2) \;=\; \frac{\partial f(P,\tilde{\theta})}{\partial\theta}\Delta\theta. \quad (62)$$

From (56) we have $\frac{\partial f}{\partial\theta}=f_1+f_2+f_3$ where we define

$$f_1 := \frac{\frac{-4}{P}h^*\sin(\theta)}{(\frac{\cos(\theta)}{2}-1)P+2h^*\sin(\theta)},$$

$$f_2 := \frac{-\cos(\theta)}{(\frac{\cos(\theta)}{2}-1)P+2h^*\sin(\theta)},$$

$$f_3 := \frac{\left(\frac{-4}{P}h^*\cos(\theta)-\sin(\theta)\right)\left(2h^*\cos(\theta)-\frac{\sin(\theta)}{2}P\right)}{\left((\frac{\cos(\theta)}{2}-1)P+2h^*\sin(\theta)\right)^2}.$$

Since $P\to 0$ implies that $\theta\to\frac{-\pi}{2}$, it follows that f_2 and f_3 are bounded by some constants, while $f_1\to-\infty$ as $P\to 0$. Thus, f_1 is the dominating term, and there exists a constant $k>0$ such that $\frac{\partial f}{\partial\theta}\leq\frac{-k}{P}$. From (62), we then have $\frac{d\Delta\theta}{dP}\leq\frac{-k}{P}\Delta\theta$, from which $\frac{d\Delta\theta}{\Delta\theta}\leq -k\frac{dP}{P}$. Solving the latter differential equation (and by Gronwall's Lemma), for any $P'<P$ we can show

$$\ln\left|\frac{\Delta\theta}{\Delta\theta'}\right|\leq -k\ln\left|\frac{P}{P'}\right| \quad\Rightarrow\quad \Delta\theta\,P^k \;\leq\; \Delta\theta'\,P'^k \quad (63)$$

where $\Delta\theta':=\Delta\theta(P')$. Since $P'\to 0$ implies that $\Delta\theta'\to 0$ as can be seen in Fig. 7, from (63) we have $\Delta\theta\,P^k\leq 0$, which implies $\Delta\theta=0$. This implies $\theta_1=\theta_2$, which is a contradiction. Therefore, there is only one trajectory for which $P\to 0$.

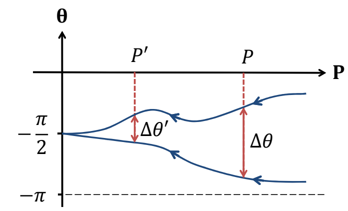

Fig. 7. Two trajectories converging to $\theta=\frac{-\pi}{2}$ as $P\to 0$.

References

[1] F. Giulietti, L. Pollini, and M. Innocenti, "Autonomous formation flight," *IEEE Control Systems*, vol. 20, no. 6, pp. 34–44, 2000.

[2] L. Y. Wang, A. Syed, G. G. Yin, A. Pandya, and H. Zhang, "Control of vehicle platoons for highway safety and efficient utility: Consensus with communications and vehicle dynamics," *Journal of systems science and complexity*, vol. 27, no. 4, pp. 605–631, 2014.

[3] A. Spröwitz, R. Moeckel, M. Vespignani, S. Bonardi, and A. J. Ijspeert, "Roombots: A hardware perspective on 3D self-reconfiguration and locomotion with a homogeneous modular robot," *Robotics and Autonomous Systems*, vol. 62, no. 7, pp. 1016–1033, 2014.

[4] Y. Cao, W. Yu, W. Ren, and G. Chen, "An overview of recent progress in the study of distributed multi-agent coordination," *IEEE Transactions on Industrial Informatics*, vol. 9, no. 1, pp. 427–438, 2013.

[5] E. Montijano, D. Zhou, M. Schwager, and C. Sagues, "Distributed formation control without a global reference frame," in *IEEE American Control Conference*, 2014, pp. 3862–3867.

[6] R. Olfati-Saber and R. M. Murray, "Distributed cooperative control of multiple vehicle formations using structural potential functions," in *IFAC World Congress*, 2002, pp. 346–352.

[7] L. Krick, M. E. Broucke, and B. A. Francis, "Stabilisation of infinitesimally rigid formations of multi-robot networks," *International Journal of Control*, vol. 82, no. 3, pp. 423–439, 2009.

[8] Y.-P. Tian and Q. Wang, "Global stabilization of rigid formations in the plane," *Automatica*, vol. 49, no. 5, pp. 1436–1441, 2013.

[9] M. H. Trinh, K.-K. Oh, and H.-S. Ahn, "Angle-based control of directed acyclic formations with three-leaders," in *International conference on mechatronics and control*, 2014, pp. 2268–2271.

[10] M. Deghat and A. N. Bishop, "Distributed shape control and collision avoidance for multi-agent systems with bearing-only constraints," in *IEEE European Control Conference*, 2015, pp. 2342–2347.

[11] S. Zhao and D. Zelazo, "Bearing rigidity and almost global bearing-only formation stabilization," *IEEE Transactions on Automatic Control*, vol. PP, no. 99, pp. 1–1, 2015.

[12] A. N. Bishop, T. H. Summers, and B. D. Anderson, "Stabilization of stiff formations with a mix of direction and distance constraints," in *IEEE International Conference on Control Applications*, 2013, pp. 1194–1199.

[13] K. Fathian, D. I. Rachinskii, M. W. Spong, and N. R. Gans, "Globally asymptotically stable distributed control for distance and bearing based multi-agent formations," in *American Control Conference*. IEEE, 2016, pp. 4642–4648.

[14] M. Basiri, A. N. Bishop, and P. Jensfelt, "Distributed control of triangular formations with angle-only constraints," *Systems & Control Letters*, vol. 59, no. 2, pp. 147–154, 2010.

[15] A. N. Bishop, "Distributed bearing-only formation control with four agents and a weak control law," in *IEEE International Conference on Control and Automation*, 2011, pp. 30–35.

[16] S. Zhao, F. Lin, K. Peng, B. M. Chen, and T. H. Lee, "Distributed control of angle-constrained circular formations using bearing-only measurements," in *IEEE Asian Control Conference*, 2013, pp. 1–6.

[17] S. L. Smith, M. E. Broucke, and B. A. Francis, "Stabilizing a multi-agent system to an equilateral polygon formation," in *International Symposium on Mathematical Theory of Networks and Systems*. Kyoto Japan, 2006, pp. 2415–2424.

[18] D. V. Dimarogonas and K. H. Johansson, "Further results on the stability of distance-based multi-robot formations," in *IEEE American Control Conference*, 2009, pp. 2972–2977.

[19] M.-A. Belabbas, "On global stability of planar formations," *IEEE Transactions on Automatic Control*, vol. 58, no. 8, pp. 2148–2153, 2013.

[20] J. A. Marshall, M. E. Broucke, and B. A. Francis, "Formations of vehicles in cyclic pursuit," *IEEE Transactions on automatic control*, vol. 49, no. 11, pp. 1963–1974, 2004.

[21] K. S. Galloway, E. W. Justh, and P. S. Krishnaprasad, "Geometry of cyclic pursuit," in *IEEE Conference on Decision and Control*, 2009, pp. 7485–7490.

[22] J. Guo, G. Yan, and Z. Lin, "Cooperative control synthesis for moving-target-enclosing with changing topologies," in *IEEE International Conference on Robotics and Automation*, 2010, pp. 1468–1473.

[23] G. Teschl, *Ordinary differential equations and dynamical systems*. American Mathematical Soc., 2012, vol. 140.

[24] A. S. Posamentier and I. Lehmann, *The secrets of triangles: a mathematical journey*. Prometheus Books, 2012.